THE KrkNLO METHOD FOR PARTON SHOWER MATCHING*

James Whitehead

Institute of Nuclear Physics Polish Academy of Sciences
Radzikowskiego 152, 31-342 Kraków, Poland

Pratixan Sarmah, Andrzej Siódmok

Institute of Applied Computer Science, Jagiellonian University
Łojasiewicza 11, 30-348 Kraków, Poland

Received 5 June 2024, accepted 11 June 2024,
published online 5 August 2024

The consistent combination of Next-to-Leading-Order (NLO) perturbative QCD with the logarithmic resummation provided by parton shower algorithms ('NLO matching') is an indispensable tool for LHC phenomenology. Two methods for achieving this have been widely adopted: Mc@Nlo and Powheg. We summarise a third method, KrkNLO, its implementation in Herwig 7, and compare the results it produces with comparable results from Mc@Nlo.

DOI:10.5506/APhysPolBSupp.17.5-A9

1. Introduction

'NLO matching' methods modify an inclusive, low-multiplicity fixed-order NLO calculation to produce predictions for exclusive high-multiplicity observables, retaining the perturbative accuracy of the former (up to power corrections) but augmenting it with the logarithmic resummation of a parton shower to provide the flexibility of exclusive predictions. The dominant, long-established methods are Mc@Nlo [1] and Powheg [2–4]. The KrkNLO method was introduced in [5–7] and uses a modified factorisation scheme, the Krk scheme, to achieve NLO accuracy via a multiplicative reweight alone. Here we summarise the method and its implementation in Herwig, and present a comparison between KrkNLO and Mc@Nlo for diphoton production.

* Presented at the 30[th] Cracow Epiphany Conference on *Precision Physics at High Energy Colliders*, Cracow, Poland, 8–12 January, 2024.

2. The KrkNLO method

The KrkNLO method [5–8] solves the NLO matching problem by exploiting the freedom to choose a parton distribution function (PDF) factorisation scheme (FS) for QCD calculations at NLO and higher. The factorisation scheme used, the Krk scheme [9], is defined by the requirement that the collinear contributions to the partonic cross section, arising for a 'dipole shower' [10, 11] from the Catani–Seymour P and K operators [12], are exactly cancelled by the choice of factorisation scheme: in effect, these terms are moved from the partonic cross section into the PDFs.

As an algorithm, the KrkNLO method may be summarised as:

---

for all Born events **do** shower
  if first emission generated, from kernel (α) **then**
    $w \leftarrow w \times \frac{R(\Phi_{m+1})}{P_m^{(\alpha)}(\Phi_{m+1})}$
  end if
  $w \leftarrow w \times \left[1 + \frac{\alpha_s(\mu_R)}{2\pi}\left(\frac{V(\Phi_m;\mu_R)}{B(\Phi_m)} + \frac{I(\Phi_m;\tilde{\mu}_R)}{B(\Phi_m)} + \Delta_0^{FS}\right)\right]$
end for

The shower is then allowed to run to completion. Further details are available in [8].

Here Φ_m denotes the Born phase-space and Φ_{m+1} the real-emission phase-space. B, R and V denote the relevant Born, real, and virtual matrix elements respectively; $P_m^{(\alpha)}$ the emission kernel used in the shower algorithm to generate the chosen branching of generalised type (α); μ_R the renormalisation scale, and I the contribution from the shower Sudakov, integrated over the radiative phase-space, containing no residual collinear dependence.

This achieves NLO accuracy if and only if convolved with PDFs in the 'Krk' factorisation scheme [9], which is defined to compensate for the additional collinear terms arising at $\mathcal{O}(\alpha_s)$ from the parton shower Sudakov factor. A detailed derivation illustrating NLO accuracy can be found in [8]. This scheme has so far been formulated only for colour-singlet final states.

In order for the full real-emission phase-space Φ_{m+1} to be populated by the reweighted first shower emission, the shower must be constructed to have full phase-space coverage (*i.e.*, no 'dead zones'). The shower starting scale must also be chosen to coincide with the maximum kinematically-attainable scale for each dipole. This can be relaxed by using the Mc@Nlo method to fill in the remaining phase-space [13].

Numerically, the KrkNLO procedure shares with Powheg the advantage of generating no negative-weighted events. These arise in the Mc@Nlo method due to its use of (potentially over-)subtracted events in the hard process. Unlike POWHEG, in KrkNLO this is achieved without requiring the modification of the shower kernel (and by consequence, the Sudakov factor) for the first parton-shower emission, the exponentiation of which has been found to be potentially problematic [14] and to require manual damping [15].

3. Implementation and validation

We have implemented the KrkNLO algorithm in Herwig 7 [16–18], a multi-purpose Monte Carlo Event Generator which, through the Matchbox module [19] provides NLO QCD predictions, matched automatically and consistently to either the dipole [11, 19] or the angular-ordered shower [20], using either the MC@NLO or POWHEG methods, within the Matchbox module [19].

For KrkNLO we use the Herwig dipole shower. The diphoton process has been implemented manually as an intermediate step to full automation; the fully-automated method, suitable for any colour-singlet final state, is being validated and is expected to be the subject of an upcoming publication.

We have validated the implementation numerically by numerically calculating, and unweighting by, the Sudakov factor generated by the veto algorithm [21–23] and comparing the resulting distributions numerically to those arising from the fixed-order real-emission matrix element. Plots illustrating excellent agreement are shown in Fig. 1. The virtual reweight can be isolated by setting the shower cut-off scale sufficiently high to prohibit all shower radiation; the matrix elements have been tested phase-space-point by phase-space-point against OpenLoops [24] and distributions corresponding to the Born and/or virtual matrix elements have been compared numerically to those calculated by Matchbox; plots illustrating excellent agreement are shown in Fig. 2.

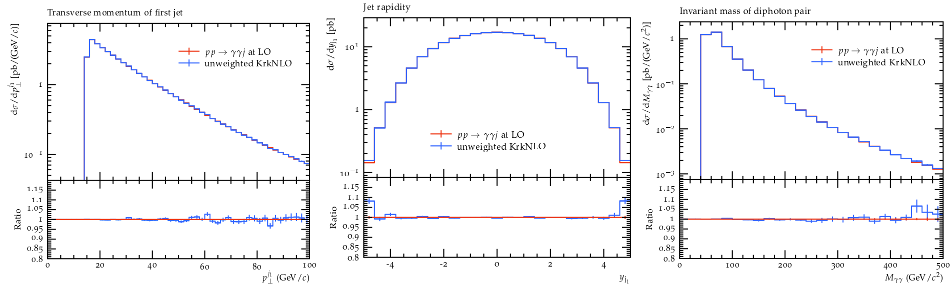

Fig. 1. Validation of the real weight by unweighting by the Sudakov factor to isolate the real matrix element within the KrkNLO implementation.

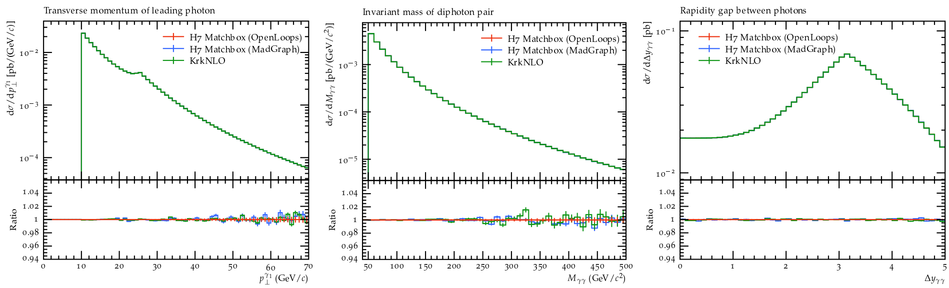

Fig. 2. Validation of the virtual weight $V + I$ for the $q\bar{q}$-channel.

4. Comparison with MC@NLO

Alternative matching methods all achieve formal NLO perturbative accuracy, but differ by formally-higher-order terms which may nevertheless be numerically significant, especially in regions of phase-space where the Sudakov factor is large (and therefore significantly different from its truncated perturbative expansion). In [8], we perform a detailed comparison of the KrkNLO method to the MC@NLO method with three different choices of shower starting-scale $Q(\Phi)$:

— a 'power-shower' with $Q(\Phi_m) = Q_{\max}(\Phi_m)$ and $Q(\Phi_{m+1}) = Q_{\max}(\Phi_{m+1})$;

— a 'default' shower with $Q(\Phi_m) = \sqrt{\hat{s}_{12}} \equiv M_{\gamma\gamma}$ and $Q(\Phi_{m+1}) = p_{\mathrm{T}}^{j_1}$, and

— a 'DGLAP-inspired' choice in which the shower starting-scale consistently matches the factorisation scale, $Q(\Phi_m) = \sqrt{\hat{s}_{12}}$ and $Q(\Phi_{m+1}) = \sqrt{\hat{s}_{12}}$.

For the KrkNLO method, the shower starting-scale is fixed to $Q_{\max}(\Phi_m)$, as required to populate the entire real-emission phase-space. Because all KrkNLO events start from a generated Born phase-space configuration, $Q(\Phi_{m+1})$ is set by the shower algorithm to $p_{\mathrm{T},1}$, the transverse momentum of the first generated emission with respect to the axis of its emitter–spectator pair, in the rest frame of the emitter–spectator pair.

Concretely, we present results with fiducial cuts close to those used by ATLAS for LHC Run 2 at 13 TeV [25]:

$$p_{\mathrm{T}}^{\gamma_1} > 40\ \mathrm{GeV}\,, \qquad p_{\mathrm{T}}^{\gamma_2} > 30\ \mathrm{GeV}\,, \tag{1a}$$

$$\Delta R_{\gamma\gamma} > 0.4\,, \qquad |y^{\gamma}| \in [0, 2.5)\,, \tag{1b}$$

$$E_{\mathrm{T}}^{\mathrm{iso,part}} < 0.1\, p_{\mathrm{T}}^{\gamma} \qquad \text{within cone } \Delta R \leqslant 0.4\,. \tag{1c}$$

In place of the experimental photon isolation, we use smooth-cone ('Frixione') isolation [26] with the 'tight' isolation parameters from the 2013 Les Houches Accords [27]. Where jet distributions are presented, we use the anti-k_{T} algorithm [28] with clustering radius of 0.4 and a p_{T} cut of 1 GeV.

We use `CT18NLO` PDFs [29], either in the $\overline{\mathrm{MS}}$ scheme or transformed into the Krk scheme; to match, we adopt $\alpha_{\mathrm{s}}(M_Z) = 0.118$ consistently throughout. We use the Herwig 7 default dipole-shower cut-off scale $p_{\mathrm{T}}^{\mathrm{cut}} = 1$ GeV. Within Herwig, we disable both hadronisation and the `RemnantDecayer` so the final-state of the hard-process is the only source of final-state QCD partons and the hard-process is the only input into the parton shower initial conditions.

In Section 4.1, we present results for the shower truncated to one emission; at this point, the role of the matching algorithm has concluded, and influences the subsequent shower evolution only through the shower starting scale for the second emission. In Section 4.2, we present results for the full shower, untruncated. A more detailed analysis including additional distributions is available in [8].

4.1. First-emission only

In the one-emission case, the shower starting-scale within Mc@Nlo for parton shower emissions from 'H'-events, $Q(\Phi_{m+1})$, does not enter the calculation, as the shower is truncated before any such emissions can be generated. In this case, the second ('default') and third ('DGLAP') choices outlined above are identical. In practice, when truncated to a single emission, the sensitivity to the different choices of $Q(\Phi_m)$ between the 'power' and 'default'/'DGLAP' alternatives are also very small (*i.e.*, within the Monte Carlo uncertainties). We therefore present only the power-shower result in this section and do not distinguish between them further.

In Fig. 3, we show the $\mathrm{d}\sigma/\mathrm{d}p_{\mathrm{T}}^{j_1}$ and $\mathrm{d}\sigma/\mathrm{d}M_{\gamma\gamma}$ distributions. We observe good agreement between the predictions, with both KrkNLO and Mc@Nlo reproducing the NLO fixed-order $p_{\mathrm{T}}^{j_1}$-distribution. At low-$p_{\mathrm{T}}^{j_1}$, the Sudakov factor from the shower emission used to populate the real-emission phase-space in the KrkNLO method leads to suppression relative to Mc@Nlo (which is already suppressed relative to the fixed-order matrix-element, which diverges in the $p_{\mathrm{T}}^{j_1} \to 0$ limit).

This can be seen in more detail double-differentially in Fig. 4, where the $\mathrm{d}\sigma/\mathrm{d}p_{\mathrm{T}}^{j_1}$ distribution is partitioned into six equal slices according to the value of $\Delta\phi_{\gamma\gamma}$. Values of $\Delta\phi_{\gamma\gamma} \approx \pi$ correspond to a Born-like configuration (in the Born kinematics, $\Delta\phi_{\gamma\gamma} = \pi$) in which the two photons are approximately back-to-back, while very small values of $\Delta\phi_{\gamma\gamma}$ imply recoil of the diphoton system against a hard jet. We see reasonable agreement across phase-space except for the effect of the Sudakov factor in close-to-Born configurations.

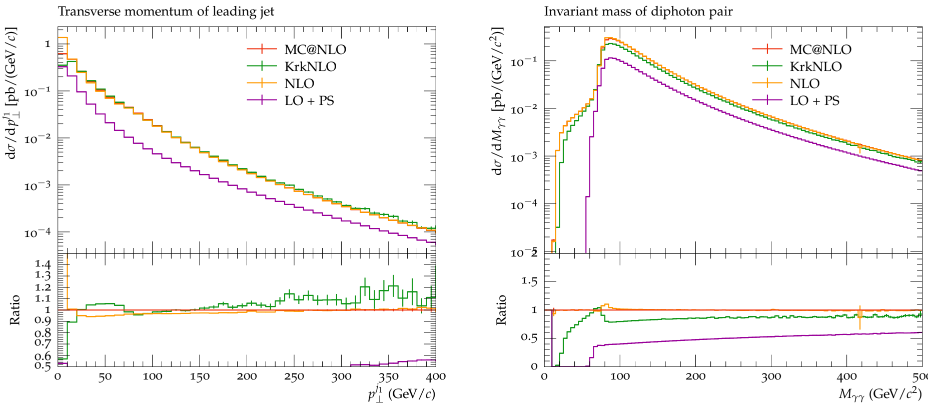

Fig. 3. ‘Parton level’ (first-emission) comparison of KrkNLO with Mc@Nlo, NLO fixed-order, and the corresponding first-emission distributions generated by the parton shower from a leading-order calculation. The shower in each case is a ‘power shower’, *i.e.* with no phase-space restrictions.

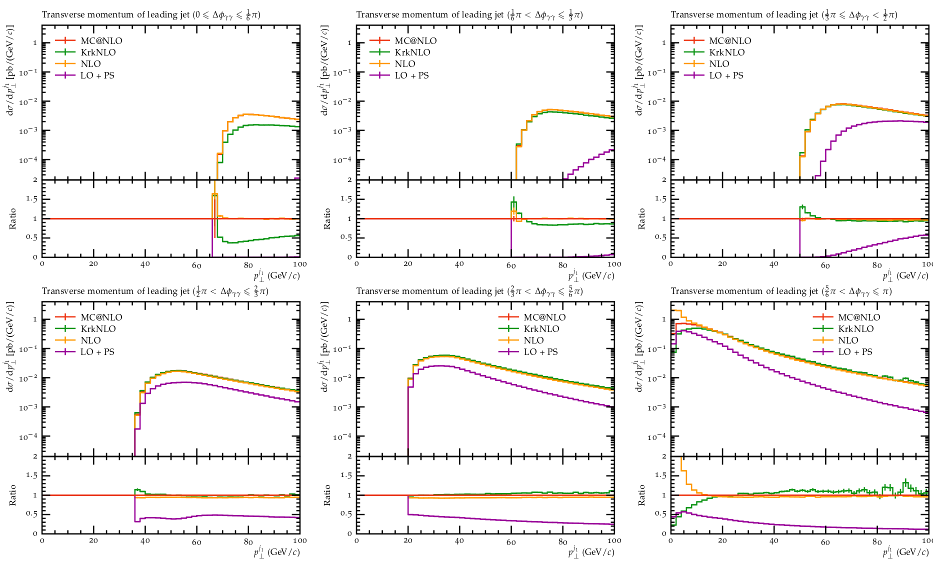

Fig. 4. ‘Parton level’ (first-emission) comparison of the transverse-momentum distribution of the hardest jet (here, also parton), $\mathrm{d}\sigma/\mathrm{d}p_{\mathrm{T}}^{j_1}$, divided into six equal bins of $\Delta\phi_{\gamma\gamma}$, generated by KrkNLO, Mc@Nlo, NLO fixed-order, and the corresponding first-emission distributions generated by the parton shower from a leading-order calculation.

The $\mathrm{d}\sigma/\mathrm{d}M_{\gamma\gamma}$ distribution shown in Fig. 3 shows agreement consistent with the NLO accuracy of the methods, with large deviations only in regions of the distribution that are accurate to leading-order only ($M_{\gamma\gamma} < 80$ GeV).

4.2. Full shower

Phenomenologically-relevant results are obtained by allowing the shower to run to completion, untruncated. The same two distributions, $\mathrm{d}\sigma/\mathrm{d}p_{\mathrm{T}}^{j_1}$ and $\mathrm{d}\sigma/\mathrm{d}M_{\gamma\gamma}$ are shown in Fig. 5. In this case, we see that, as expected, the 'power' shower favours the emission of considerably harder jets than the other options. The KrkNLO distribution is closest to the Herwig 'default' shower, and lies between the 'default' and 'DGLAP' scale choices. The $\mathrm{d}\sigma/\mathrm{d}M_{\gamma\gamma}$ distributions are in excellent agreement with each other, as might be hoped, with disagreement again only in the effectively-leading-order region of $M_{\gamma\gamma} < 80$ GeV. The variable $M_{\gamma\gamma}$ is privileged to some extent in all matching methods since it is preserved by the shower momentum mappings, through its relationship to the Lorentz invariant $s_{\gamma\gamma} = M^2_{\gamma\gamma}$.

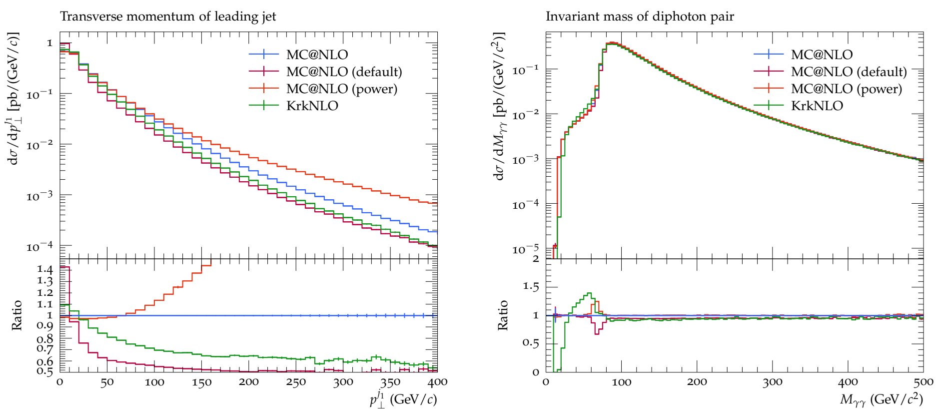

Fig. 5. Comparison of matched differential cross sections generated by KrkNLO and Mc@Nlo with the 'default', 'power'-shower and 'DGLAP' starting-scales.

Looking at $\mathrm{d}\sigma/\mathrm{d}p_{\mathrm{T}}^{j_1}$ double-differentially in slices of $\Delta\phi_{\gamma\gamma}$ in Fig. 6, we again see reasonably good agreement between the methods across phase-space. In general, the KrkNLO distributions lie within the intrinsic uncertainty spanned by the variation of the shower starting-scale within the Mc@Nlo method, lying closest to the Herwig 'default' scale choice and generally between the Herwig 'default' and the 'DGLAP' choices.

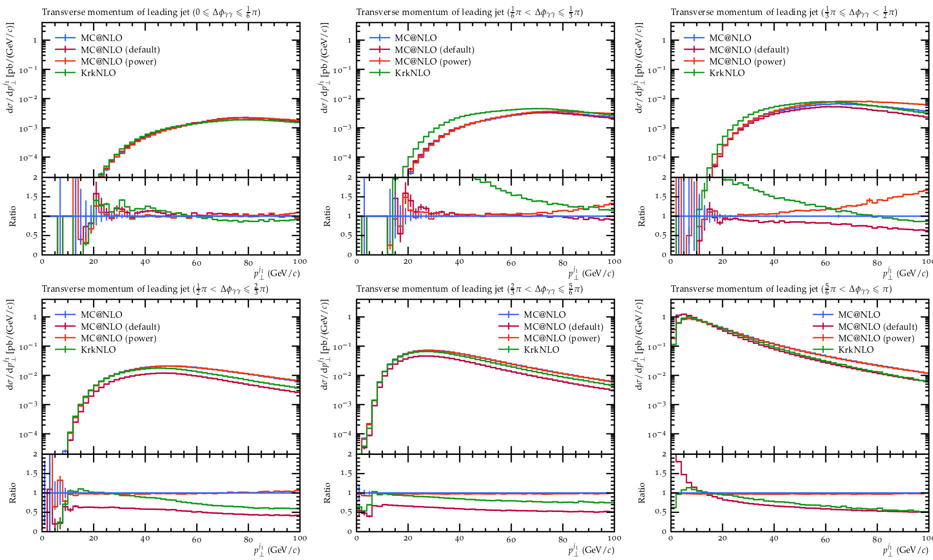

Fig. 6. Comparison of matched differential cross-sections of the transverse-momentum distribution of the hardest jet, $\mathrm{d}\sigma/\mathrm{d}p_{\mathrm{T}}^{j_1}$, divided into six equal bins of $\Delta\phi_{\gamma\gamma}$, generated by KrkNLO and Mc@Nlo with the 'default', 'power'-shower and 'DGLAP' starting-scales.

5. Conclusions

In these proceedings, we have summarised the KrkNLO method and outlined the results of the comparison performed between KrkNLO and Mc@Nlo matching in [8]. We have further demonstrated that KrkNLO is capable of producing NLO matched results which lie within the wide scale-variation band spanned by reasonable choices of scale for one of the main established alternative methods, Mc@Nlo, and are qualitatively close to Mc@Nlo when combined with a common choice of shower starting scale. Since KrkNLO has no shower-scale parameter to vary, it provides a valuable independent indication of the matching uncertainty associated with the choices of scales within Mc@Nlo (analogously, the choice of damping function/parameters in Powheg).

With the forthcoming publication and public release of the KrkNLO code within Herwig 7, we hope to demonstrate that KrkNLO is a competitive method for practical LHC phenomenology, at least for the production of colour-singlet final-states. We intend to pursue further work studying the implications of the KrkNLO method for other such processes, with further comparisons to Mc@Nlo. We remain optimistic about the applicability of a variant of the KrkNLO method to more complex processes and higher-orders.

The authors wish to thank Wiesław Płaczek and the late Stanisław Jadach for their work on, and for many fruitful discussions about, the KrkNLO method, and Simon Plätzer for productive discussions about NLO matching and for his insight into and assistance with Herwig and Matchbox. This work was supported by grant 2019/34/E/ST2/00457 of the National Science Centre (NCN), Poland. A.S. is also supported by the Priority Research Area Digiworld under the program 'Excellence Initiative — Research University' at the Jagiellonian University in Kraków. We gratefully acknowledge the Polish high-performance computing infrastructure PLGrid (HPC Centre: ACK Cyfronet AGH) for providing computing facilities and support within computational grant PLG/2023/016494.

REFERENCES

[1] S. Frixione, B.R. Webber, *J. High Energy Phys.* **2002**, 029 (2002), `arXiv:hep-ph/0204244`.

[2] P. Nason, *J. High Energy Phys.* **2004**, 040 (2004), `arXiv:hep-ph/0409146`.

[3] S. Frixione, P. Nason, C. Oleari, *J. High Energy Phys.* **2007**, 070 (2007), `arXiv:0709.2092 [hep-ph]`.

[4] S. Alioli, P. Nason, C. Oleari, E. Re, *J. High Energy Phys.* **2010**, 043 (2010), `arXiv:1002.2581 [hep-ph]`.

[5] S. Jadach *et al.*, *Phys. Rev. D* **87**, 034029 (2013), `arXiv:1103.5015 [hep-ph]`.

[6] S. Jadach *et al.*, *J. High Energy Phys.* **2015**, 052 (2015), `arXiv:1503.06849 [hep-ph]`.

[7] S. Jadach *et al.*, *Eur. Phys. J. C* **77**, 164 (2017), `arXiv:1607.06799 [hep-ph]`.

[8] P. Sarmah, A. Siódmok, J. Whitehead, «KrkNLO matching for colour-singlet processes», to be submitted to *J. High Energy Phys.*, 2024.

[9] S. Jadach *et al.*, *Eur. Phys. J. C* **76**, 649 (2016), `arXiv:1606.00355 [hep-ph]`.

[10] M. Dinsdale, M. Ternick, S. Weinzierl, *Phys. Rev. D* **76**, 094003 (2007), `arXiv:0709.1026 [hep-ph]`.

[11] S. Schumann, F. Krauss, *J. High Energy Phys.* **2008**, 038 (2008), `arXiv:0709.1027 [hep-ph]`.

[12] S. Catani, M.H. Seymour, *Nucl. Phys. B* **485**, 291 (1997), `arXiv:hep-ph/9605323`.

[13] P. Nason, G.P. Salam, *J. High Energy Phys.* **2022**, 067 (2022), `arXiv:2111.03553 [hep-ph]`.

[14] S. Höche, F. Krauss, M. Schönherr, F. Siegert, *J. High Energy Phys.* **2012**, 049 (2012), `arXiv:1111.1220 [hep-ph]`.

[15] S. Alioli, P. Nason, C. Oleari, E. Re, *J. High Energy Phys.* **2009**, 002 (2009), arXiv:0812.0578 [hep-ph].
[16] J. Bellm *et al.*, *Eur. Phys. J. C* **76**, 196 (2016), arXiv:1512.01178 [hep-ph].
[17] J. Bellm *et al.*, *Eur. Phys. J. C* **80**, 452 (2020), arXiv:1912.06509 [hep-ph].
[18] G. Bewick *et al.*, arXiv:2312.05175 [hep-ph].
[19] S. Plätzer, S. Gieseke, *Eur. Phys. J. C* **72**, 2187 (2012), arXiv:1109.6256 [hep-ph].
[20] S. Gieseke, P. Stephens, B. Webber, *J. High Energy Phys.* **2003**, 045 (2003), arXiv:hep-ph/0310083.
[21] M.H. Seymour, *Comput. Phys. Commun.* **90**, 95 (1995), arXiv:hep-ph/9410414.
[22] T. Sjöstrand, S. Mrenna, P.Z. Skands, *J. High Energy Phys.* **2006**, 026 (2006), arXiv:hep-ph/0603175.
[23] S. Plätzer, M. Sjödahl, *Eur. Phys. J. Plus* **127**, 26 (2012), arXiv:1108.6180 [hep-ph].
[24] F. Buccioni *et al.*, *Eur. Phys. J. C* **79**, 866 (2019), arXiv:1907.13071 [hep-ph].
[25] ATLAS Collaboration (G. Aad *et al.*), *J. High Energy Phys.* **2021**, 169 (2021). arXiv:2107.09330 [hep-ex].
[26] S. Frixione, *Phys. Lett. B* **429**, 369 (1998), arXiv:hep-ph/9801442.
[27] J.R. Andersen *et al.*, arXiv:1405.1067 [hep-ph].
[28] M. Cacciari, G.P. Salam, G. Soyez, *J. High Energy Phys.* **2008**, 063 (2008), arXiv:0802.1189 [hep-ph].
[29] T.-J. Hou *et al.*, *Phys. Rev. D* **103**, 014013 (2021), arXiv:1912.10053 [hep-ph].